# Modeling and Optimization of Microwave Devices and Circuits Using Genetic Algorithms

Yasser A. Hussein, *Member, IEEE,* and Samir M. El-Ghazaly, *Fellow, IEEE*

***Abstract*—This paper presents a new approach for the simulation and optimization of microwave devices using a genetic algorithm (GA). The proposed technique solves the equations that describe the semiconductor transport physics in conjunction with Poisson's equation, employing an adaptive real-coded GA. An objective function is formulated, and most of the GA parameters are recommended to change during the simulation. In addition, different methods for describing the way the GA parameters change are developed and studied. The effect of GA parameters including the mutation value, number of crossover points, selection criteria, size of population, and probability of mutation is analyzed. The technique is validated by simulating a submicrometer field-effect transistor, and then compared to successive over relaxation, showing the same degree of accuracy along with a moderate speed of convergence. The purpose of this paper is to introduce a new vision for a GA capable of optimizing real value functions with a considerably large number of variables. This paper also represents a fundamental step toward applying GAs to Maxwell's equations in conjunction with the hydrodynamic model, aiming to develop an optimized and unconditionally stable global-modeling simulator.**

***Index Terms*—Full hydrodynamic model (HDM), genetic algorithms (GAs), global modeling, microwave devices, optimization.**

## I. Introduction

CONTEMPORARY high-performance electronics are based on technologies such as monolithic microwave integrated circuits (MMICs) with a large number of closely packed passive and active structures, several levels of transmission lines and discontinuities, all operating at high speeds, frequencies, and sometimes over very broad bandwidths. It is thus anticipated that the design of MMICs should involve robust design tools that would simulate all the circuit elements simultaneously. The possibility of achieving this type of modeling is addressed by global circuit modeling that has been demonstrated in [1]–[4].

Global modeling is a tremendous task that involves advanced numerical techniques and different algorithms with tight stability constraints [3]. Thus, there is an urgent need to develop and present new simulation approaches that could relax or even eliminate these constraints. On the other hand, genetic algorithms (GAs) are numerical optimization algorithms inspired by both natural selection and natural genetics, which are unconditionally stable. The method is a general one, capable of being applied to an extremely wide range of problems. GAs have proven themselves for optimizing many large and complex problems in our field [5]–[11].

Some optimization problems have multiple local minima, where methods based on steepest descent would fall in one of these local minima, resulting in a different solution. GAs are random algorithms and researchers have found their generality and that they are unconditionally stable. GAs are thus suitable to find the global solution for problems having multiple minima [12]. Furthermore, in many problems involving systems of linear equations $Ax = b$, the matrix $A$ has a large condition number. For these problems, standard methods will not be able to get the correct solution. For instance, solving Poisson's equation on a nonuniform grid. In this case, genetic-based algorithms should outperform standard methods. This is because standard methods work fine only for well-posed problems (problems with the matrix $A$ having a small condition number). On the other hand, a genetic-based algorithm will converge independently of the condition number of the matrix $A$.

From the above, it is motivating to make an effort to apply GAs to Maxwell's equations or the hydrodynamic model (HDM), aiming to develop an optimized and unconditionally stable algorithm. It is noteworthy to say that the main purpose of this paper is to lay the foundation of a GA capable of optimizing real value problems with a considerably large number of unknowns.

In this stage of the study, we will demonstrate that GAs can be applied to the HDM in conjunction with Poisson's equation to accurately model submicrometer gate devices with less stability constraints. Ultimately, an HDM should be implemented with equations that would have numerical stability restrictions such as Maxwell's equations rather than Poisson's equation in order to obtain a self-consistent simulation of electromagnetic-wave propagation effects, employing an optimized and unconditionally stable algorithm.

This paper is organized as follows. Section II describes the problem under consideration. Section III presents in details the implementation of the proposed algorithm. Results along with illustrative graphs are provided in Section IV. Finally, conclusions are presented in Section V.

## II. Problem Description

The transistor model used in this study is a two-dimensional (2-D) full-hydrodynamic large-signal physical model. The ac-

Manuscript received January 19, 2003; revised April 30, 2003. This work was supported by the U.S. Army Research Office under Contract DAAD-19-99-1-0194.

Y. A. Hussein was with the Department of Electrical Engineering, Arizona State University, Tempe, AZ 85287 USA. He is now with the Stanford Linear Accelerator Center, Stanford University, Menlo Park, CA 94025 USA (e-mail: yasser@slac.stanford.edu).

S. M. El-Ghazaly is with the Department of Electrical and Computer Engineering, University of Tennessee, Knoxville, TN 37996 USA (e-mail: el-ghazaly@utk.edu).

Digital Object Identifier 10.1109/TMTT.2003.820899

tive device model is based on the moments of the Boltzmann's transport equation (BTE) obtained by integrating over the momentum space. The integration results in a strongly coupled highly nonlinear set of partial differential equations called the conservation equations. These equations provide a time-dependent self-consistent solution for carrier density, carrier energy, and carrier momentum, which are given as follows.

- *Current continuity*

$$\frac{\partial n}{\partial t} + \nabla \cdot (n\nu) = 0. \tag{1}$$

- *Energy conservation*

$$\frac{\partial (n\varepsilon)}{\partial t} + qn\nu \cdot \boldsymbol{E} + \nabla\big(n\nu(\varepsilon + K_B T)\big) = -\frac{n(\varepsilon - \varepsilon_0)}{\tau_{\varepsilon(\varepsilon)}}. \tag{2}$$

- *$x$-momentum conservation*

$$\frac{\partial (np_x)}{\partial t} + qnE_x + \frac{\partial}{\partial_x}(np_x\nu_x + nK_BT) = -\frac{n(p_x - P_0)}{\tau_m(\varepsilon)}. \tag{3}$$

In the above equations, $n$ is the electron concentration, $\nu$ is the electron velocity, $\boldsymbol{E}$ is the electric field, $\varepsilon$ is the electron energy, $\varepsilon_0$ is the equilibrium thermal energy, and $p$ is the electron momentum. The energy and momentum relaxation times are given by $\tau_\varepsilon$ and $\tau_m$, respectively. Similar expression can be obtained for the $y$-direction momentum. The three conservation equations are solved in conjunction with Poisson's equation

$$\nabla^2 \varphi = \frac{q}{\epsilon}(N_d - n) \tag{4}$$

where $\varphi$ is the electrostatic potential, $q$ is the electron charge, $\epsilon$ is the dielectric constant, $N_d$ is the doping concentration, and $n$ is the carrier concentration at any given time. The total current density distribution $\boldsymbol{J}$ inside the active device at any time $t$ is given as

$$\boldsymbol{J}(t) = -qn\nu(t). \tag{5}$$

The low field mobility is given by the empirical relation [13]

$$\mu_0 = \frac{8000}{1 + (N_d \cdot 10^{-17})^{0.5}} \left(\frac{\text{cm}^2}{\text{V} \cdot \text{s}}\right). \tag{6}$$

On the other hand, the mobility for large-signal simulations is calculated as $\mu = \nu_d / E_{ss}$, where $\nu_d$ is estimated using (7) as follows:

$$\nu_d = \frac{\mu_0 E_{ss} + \nu_{ss}\left(\dfrac{E_{ss}}{4500}\right)^6}{1 + \left(\dfrac{E_{ss}}{4500}\right)^6}. \tag{7}$$

In the above equation, $\nu_d$ is the electron drift velocity, $\mu_0$ is low field mobility given by (6), and $\nu_{ss}$ and $E_{ss}$ are the steady-state electron velocity and electric field, respectively. It is significant to note that both $\nu_{ss}$ and $E_{ss}$ are functions of energy, and they get updated each time a new energy distribution is estimated using the HDM.

The above model accurately describes all the nonstationary transport effects by incorporating energy dependence into all the transport parameters such as the effective mass and relaxation times. Fig. 1 shows the cross section of the simulated structure.

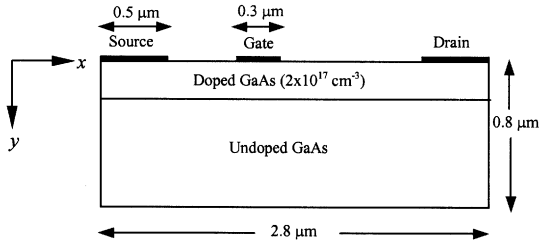


Fig. 1. Cross section of the simulated transistor.

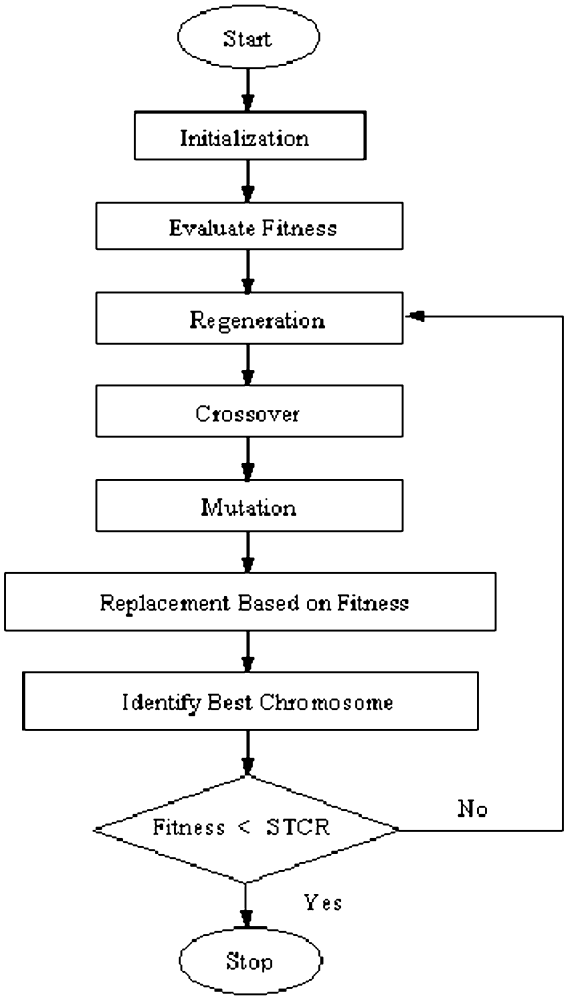


Fig. 2. Generic flowchart of the GA.

## III. Optimization Using GAs

In this section, we apply a GA for the solution of the boundary value problem for the distribution of potential across a field-effect transistor (FET).

A generic flowchart of the algorithm is shown in Fig. 2. The first step is to read the matrix $A$ and vector $b$ of the system of linear equations $Ax = b$, which are derived from Poisson's equation [14]. A population of random solutions (chromosomes) representing the vector solution $x$ is then initialized. Next, the objective function (fitness) is estimated for all the

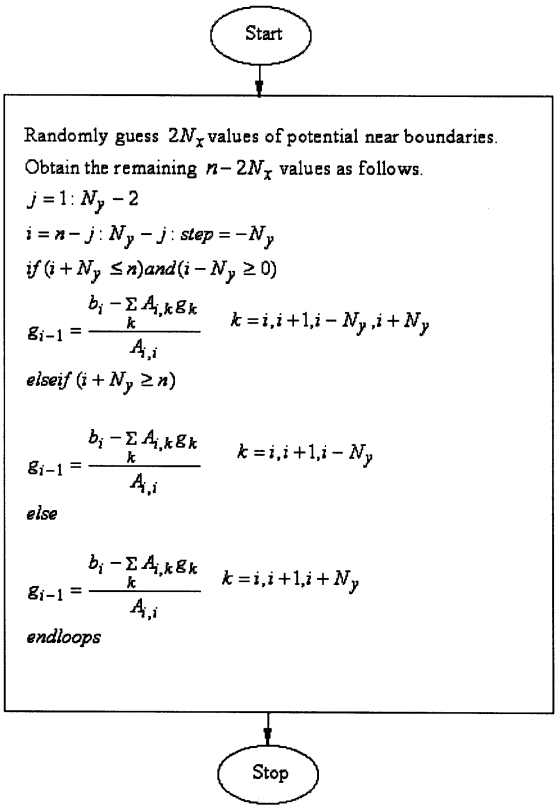


Fig. 3. Flowchart of the randomly generated solution G.

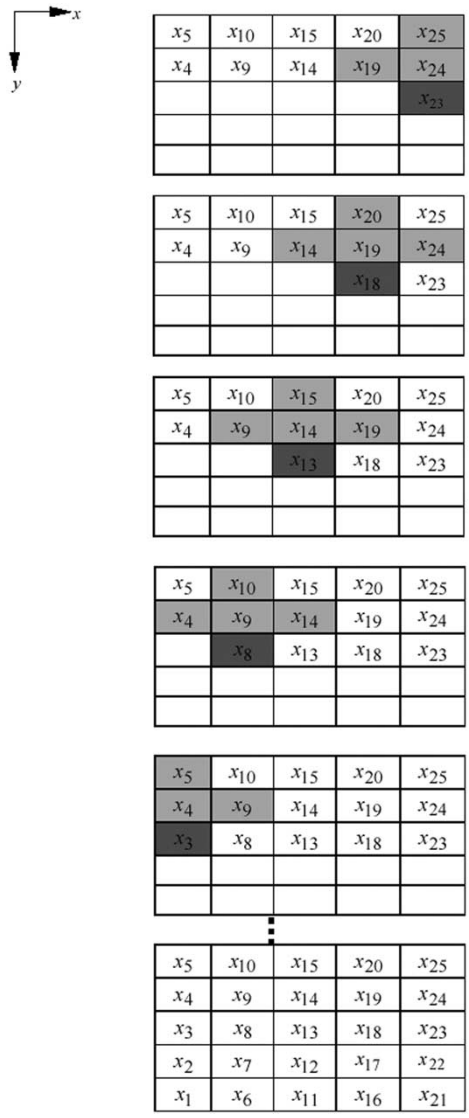


Fig. 4. $5 \times 5$ grid example illustrating how the algorithm in Fig. 3 works.

chromosomes that have been randomly generated. Based on the fitness, two parents are generated either by *roulette-wheel* or by *tournament selection* methods. Mutation and crossover are then performed on the selected parents to generate two children. Replacement is conducted by comparing the fitness of children with their parents, and the worst two chromosomes are removed from the population. The best chromosome is identified based on fitness and, finally, a check is carried out against a certain stopping criteria to either stop the simulator or to perform another iteration. The details of implementing the proposed algorithm are as follows.

*Step 1: Initialization*

Initialization is done by randomly generating $M$ chromosomes representing the GA population. Real encoding is adopted for our problem. Each chromosome contains $n$ genes, which correspond to the variables in the vector solution $x$. The generated random numbers have a range associated with the applied dc voltages to the device electrodes.

*Step 2: Evaluate Fitness*

Each chromosome is evaluated based on an objective function. The objective function is developed in a way that it accurately determines how close the randomly generated solutions are to the optimal solution.

Dealing with 2-D Poisson's equation means that the matrix $A$ has 1–5 elements in each row (sparse matrix) [14]. Based on this, it was found that the vector solution $x$ with size $n = N_x N_y$ can be fully constructed by knowing only the $2N_x$ elements close to the electrodes following the flowchart given in Fig. 3. Fig. 4 shows a simple example to illustrate the implementation of the algorithm shown in Fig. 3. Fig. 4 shows a $5 \times 5$ grid example. Each square in Fig. 4 represents a grid point. In Fig. 4, the elements in the gray squares, which represent our variables, are used to estimate the next element, which is in the darker square. For instance, the element $x_{23}$ is estimated as a linear combination of $x_{19}$, $x_{24}$, and $x_{25}$, following the algorithm in Fig. 3. This process is repeated until all the elements in our domain are estimated, as shown in Fig. 4. It is worth mentioning that the proposed numbering sequence is crucial for the correct estimation. On the other hand, the $2N_x$ elements needed to implement the algorithm in Fig. 3 can be randomly generated with a minimal error based on the following. Since boundary conditions must be satisfied, then the values of the potential are known precisely at the boundaries. Moreover, an estimate for the value of the potential near boundaries can be randomly generated bearing in mind that they would have very close values to the potential at the electrodes. The randomly generated solution $g$ along with the second norm of $Ax - b$ are included in the objective function given by (8), which needs to be maximized for a minimum

value of the dominator. In (8), $g$ is the randomly generated solution, while $\alpha$ is a scalar representing the weight of the norm criterion. The value of $\alpha$ used in the simulation is 10%.

$$\text{Fitness} = \frac{1}{1+\alpha^{-1}\sqrt{\sum_{i=1}^{n} c_i^2} + D} \tag{8}$$

where

$$D = \frac{\sum_{i=1}^{n} |x_i - g_i|}{n}$$

$$C_i = \sum_{j=1}^{n} A_{i,j}x_j - b_i.$$

*Step 3: Regeneration*

Two methods are used for parent regeneration, namely, *roulette-wheel* and *tournament* selections. The details of implementing each method are described below.

### A. Roulette-Wheel Selection

Parents in the *roulette-wheel* method are chosen randomly according to their fitness. As the name implies, the method imitates the *roulette-wheel* game, where the thrown dice would most probably end being in the slot with the largest area. Following this, one can conclude that the chromosome with the largest fitness value is most likely to be chosen because it has the largest slot size.

### B. Tournament Selection

In this method, two groups from the population are randomly selected (sub-populations). It is worth mentioning that the population size is chosen randomly as well. The best chromosome from each of the randomly generated sub-populations is chosen to represent a parent.

*Step 4: Crossover*

Now, two parents have been selected for their genes to be crossed over and mutated. Crossover is conducted by first randomly selecting a crossover point within the chromosome. Two children are then conceived by mixing the genes of the two parents at the crossover point. At this moment, two different parameters can be analyzed. The first parameter is the number of crossover points, i.e., more than one crossover point can be achieved. The other parameter is the number of genes involved in each crossover point, and will be denoted by the crossover width. The effects of both parameters are studied and included in the results section.

*Step 5: Mutation*

Mutation is carried out by randomly changing one or more genes (variables) of the created offspring. We then have two mutation parameters to study their effect. The first one is the number of mutated genes (variables) within the chromosome. The other parameter deals with the value of mutation.

TABLE I
GA PARAMETERS USED IN THE SIMULATION

| | |
|---|---|
| MU | Mutation factor or value |
| NC | Number of crossover points |
| CW | Crossover width |
| NM | Number of mutated variables |
| SC | Selection criterion |
| NPOP | Size of population |
| PM | Probability of mutation |

*Step 6: Replacement*

Replacement is performed by comparing the fitness of the parents with their offspring. The best two chromosomes out of the four are included in the population for the next iteration.

*Step 7: Ending the Algorithm*

The best chromosome is identified at each iteration and error is calculated as the second norm of $Ax-b$. This error is checked against a predefined value; if satisfied, the simulator stops and prints the final results.

## IV. RESULTS AND DISCUSSIONS

In this section, the effect of different GA parameters on the algorithm behavior is investigated. The GA parameters used in the simulation are summarized in Table I.

The default values are 0.1, 1, 1, 1, 1, 100, and 1 for MU, NC, CW, NM, SC, NPOP, and PM, respectively.

It is worth mentioning here that the developed algorithm is implemented as a subroutine to solve the system of linear equations $Ax = b$. Poisson's equation is then coupled to the HDM equations as a subroutine. The coupling is carried out as follows. First, the hydrodynamic equations are solved to get the updated value for carrier density $n$. The updated carrier density is then plugged into Poisson's equation, resulting in a new system of linear equations. The new system of linear equations is passed to the genetic-based Poisson solver to solve for $x$, i.e., the updated value of the potential. The potential is differentiated to get the electric field. Finally, the updated value of the electric field is plugged into the HDM to estimate the updated value of the carrier density. This process is repeated until the stopping criterion is satisfied.

Fig. 5 shows the distance from the optimal solution versus number of generations for different values of MU. The mutation value of any gene (variable) is proposed as follows.

$$\text{child}_{\text{new}}(i) = \text{child}_{\text{old}}(i) + \text{MU} \cdot \text{RND} \tag{9}$$

where MU is the mutation factor and RND is a random number from $-1$ to 1. Fig. 5 shows that the best result is obtained when the mutation value is fitness dependent. The reason is that as the value of the fitness increases, which indicates being very close to the optimal solution, the mutation factor decreases. In this manner, the mutation value is changed in the correct way for a faster convergence. Moreover, introducing a random feature along with the dependence of MU on the fitness does not enhance the convergence. A general conclusion is that smaller values of MU are observed to have better convergence curves.

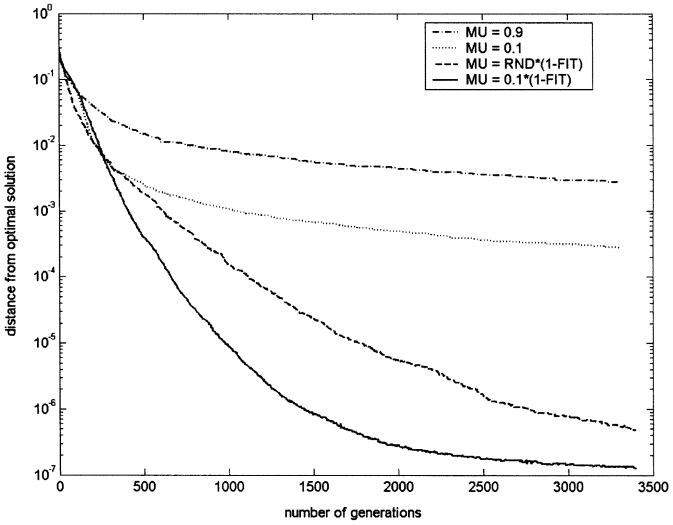


Fig. 5. Distance from the optimal solution versus number of generations for different mutation values.

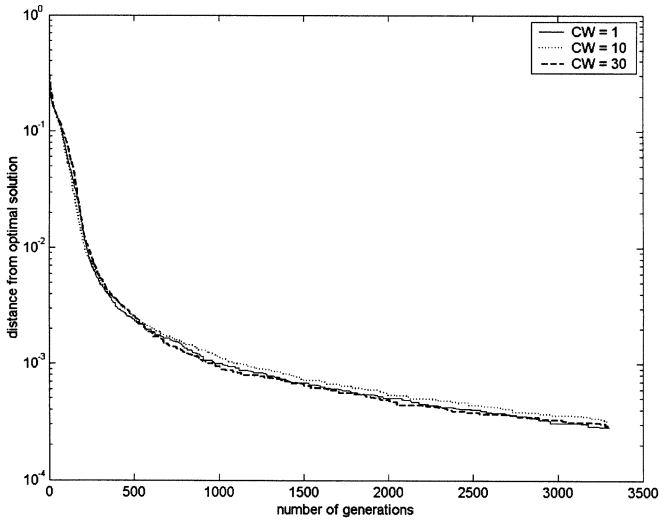


Fig. 7. Distance from the optimal solution versus number of generations for different values of crossover widths.

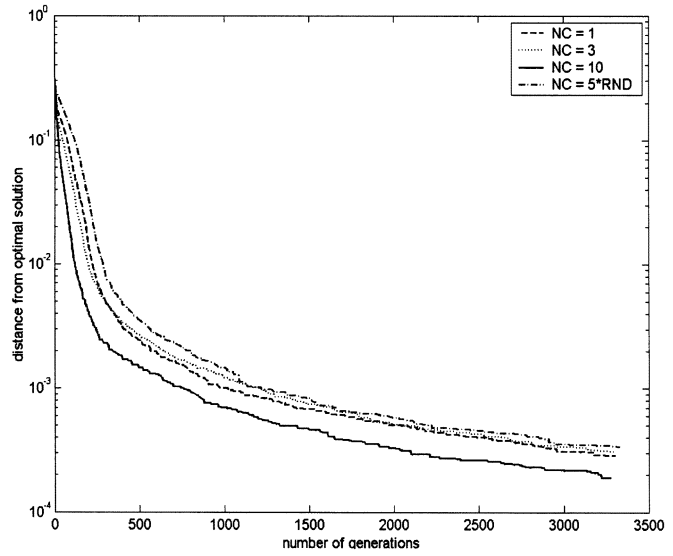


Fig. 6. Distance from the optimal solution versus number of generations for different number of crossover points.

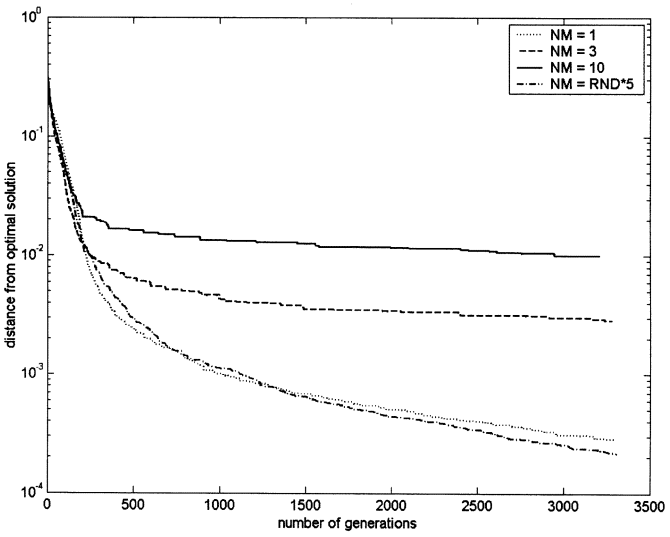


Fig. 8. Distance from the optimal solution versus number of generations for different numbers of mutated elements.

Figs. 6 and 7 illustrate the effect of the number of crossover points and crossover width, respectively. From Fig. 6, it can be concluded that larger number of crossover points is the right choice for better accuracy along with higher speed of convergence. Moreover, choosing the number of crossover points to change randomly within simulation does not improve the algorithm. On the other hand, considering Fig. 7, it is apparent that rate of convergence of the GA is independent of the crossover-width value.

Fig. 8 shows the effect of the number of mutated elements on the convergence and accuracy of the proposed algorithm. It can be observed that as the number of the mutated variables decreases, the convergence and accuracy of the algorithm are improved. The best curve is obtained for a number of mutated variables equals to 1%. This complies with nature since biological mutation hits only a very small number of genes. Moreover, changing the number of the mutated variables randomly throughout the simulation introduces a reasonable improvement over the 1% mutation case.

Fig. 9 demonstrates how the choice of the parent selection method affects the algorithm performance. It can be pointed out that *roulette-wheel selection* has the best performance. Furthermore, employing a hybrid technique does not improve the algorithm. For instance, error reaches $10^{-3}$ in almost 500 generations when *roulette-wheel selection* is employed, whereas 1200 generations are needed for *tournament selection* to reach the same value of error. It is worth mentioning here that *roulette-wheel selection* inherently uses some sort of *elitism*. Employing *elitism* may or may not be useful depending on the problem under consideration. The main reason for *roulette-wheel selection* producing better results is the choice of the objective function given by (8). It is important to mention that *tournament selection* is known to produce better results over the *roulette-wheel* method. However, this is not general, and the numerical example provided in this paper emphasizes that.

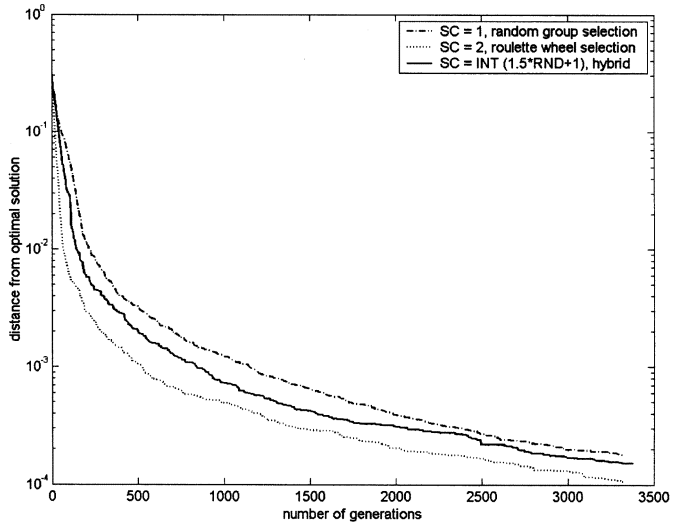


Fig. 9. Distance from the optimal solution versus number of generations for different selection criteria.

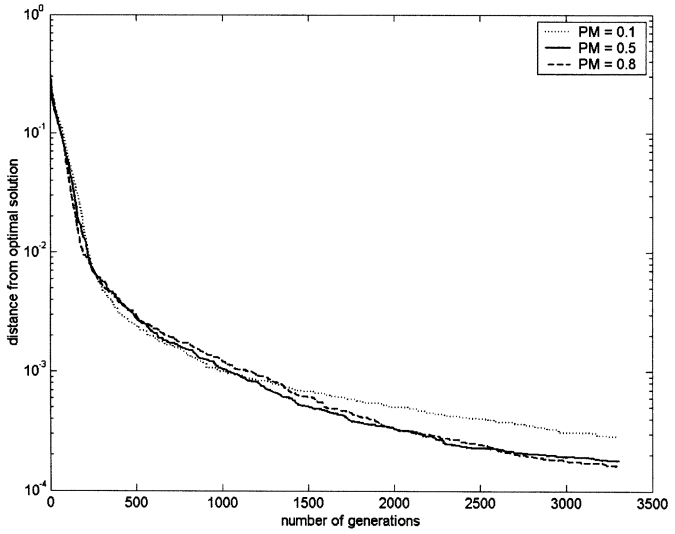


Fig. 10. Distance from the optimal solution versus number of generations for different probabilities of mutation.

Fig. 10 shows the effect of the probability of mutation. It should be noticed that increasing the probability of mutation has a positive effect on the performance of the algorithm, and the mutation probability is not crucial to the algorithm as long as it is relatively high. Fig. 11 shows the effect of the population size on the algorithm convergence. This figure emphasizes that the population size is not a critical parameter. The reason is that the proposed objective function given by (8) allows *elitism*. This makes the GA independent of the population size.

### A. DC Simulation Results

To demonstrate the potential of the proposed approach, it is applied to an idealized MESFET structure, which is discretized by a mesh of $32\Delta x \times 32\Delta y$ with $\Delta t = 0.0001$ ps. Forward Euler is adopted as an explicit finite-difference method. In addition, upwinding is employed to have a stable scheme. The space-step sizes are adjusted to satisfy Debye length, while the time-step value $\Delta t$ is chosen to satisfy the Courant–Friedrichs–Lewy (CFL) condition, while, Poisson's equation is solved using the proposed algorithm.

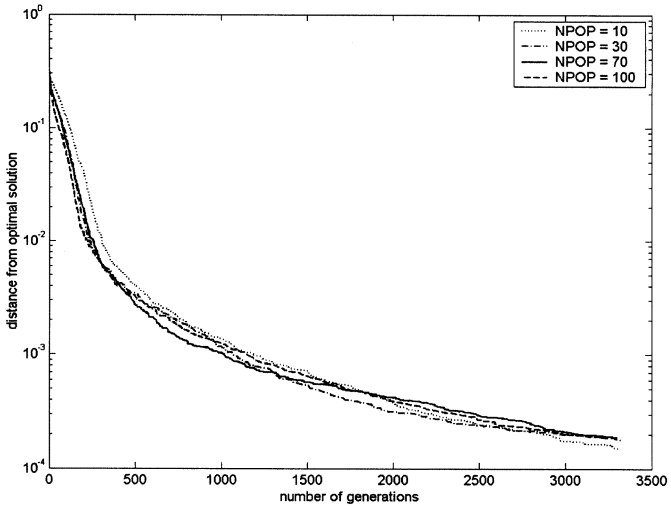


Fig. 11. Distance from the optimal solution versus number of generations for different population sizes.

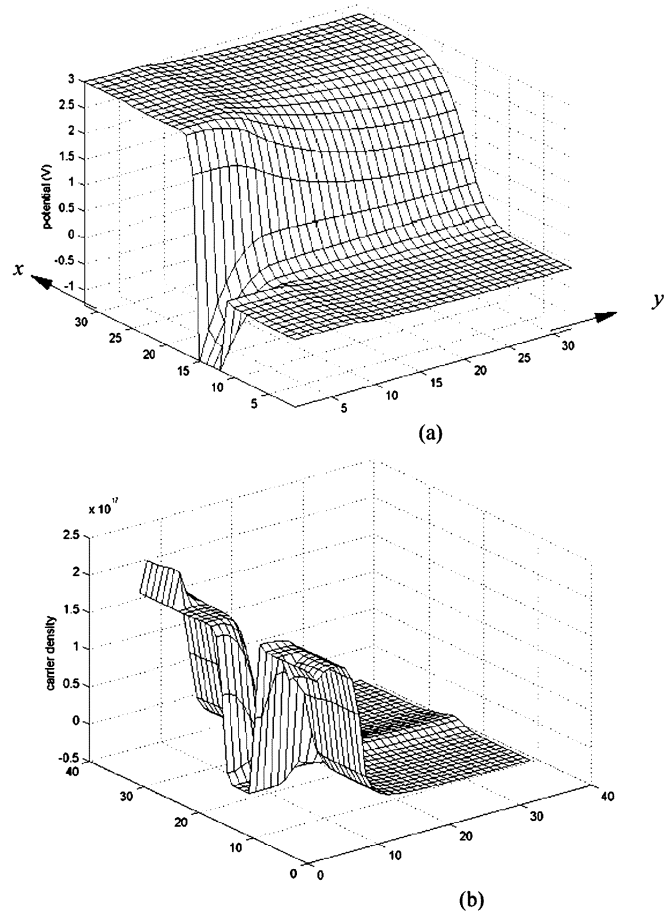


Fig. 12. Sample dc results obtained using the proposed algorithm. (a) Potential distribution. (b) Carrier-density distribution.

Fig. 12(a) shows the potential distribution obtained using the proposed algorithm. This graph demonstrates that boundary conditions are satisfied at the electrodes. For instance, the value of the potential at the gate equals to $-1.3$ V, which is the

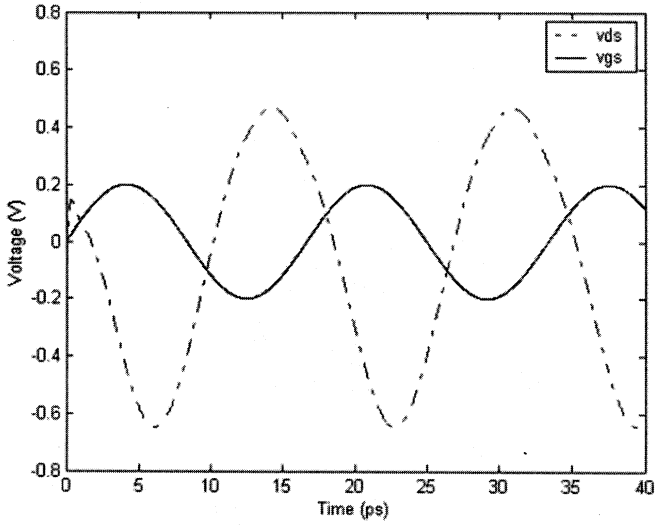


Fig. 13. AC gate and drain voltages obtained using the proposed algorithm.

applied dc voltage minus the Schottky barrier height, while, Fig. 12(b) shows the carrier-density distribution. It is significant to indicate that the proposed algorithm gives precisely the same results obtained when the successive over-relaxation (SOR) algorithm is employed. The comparison results between the algorithms are not provided because their results coincide exactly on each other. It is worth mentioning here that the purpose of this section is to show that GAs can be applied to solve real value problems having a large number of unknowns with a very high degree of accuracy. The speed of convergence is not an objective at this stage of the study. Ultimately, the developed GA needs to be applied to equations that have stability constraints in order to have unconditionally stable algorithm or to solve problems that traditional optimization techniques cannot solve (problems with multiple local minima).

### B. AC Simulation Results

The ac excitation applied to the gate electrode is given as

$$V_{\rm gs}(t) = V_{\rm gs0} + \Delta\nu_{\rm gs}\sin(\omega t) \tag{10}$$

where $V_{\rm gs}$ is the dc bias applied to the gate electrode, $\Delta\nu_{\rm gs}$ is the peak value of the ac signal (0.2 V), and $\omega$ is the frequency of the applied signal in radians per second. The frequency used in the simulation is 60 GHz.

First, the dc distribution is obtained by solving Poisson's equation using the proposed algorithm in conjunction with the three hydrodynamic conservation equations. A new value of $V_{\rm gs}$ is then calculated using (10). The new value of $V_{\rm gs}$ is used to update Poisson's equation and get the new voltage distribution. The electric field is then estimated and used to update the variables in the conservation equations. This process is repeated every $\Delta t$ until $t = t_{\max}$. The current density is obtained using (5). The current density calculated on the plan located midway between the drain and gate is integrated to obtain the total current. The output voltage is estimated by multiplying the total current by the resistance that defines the dc operating point ($Q$ point) of the transistor. Fig. 13 shows the ac gate and drain voltages. A maximum gain of 9 dB is achieved. Moreover, it is observed that there is an output delay of approximately 1 ps that represents the time required for the transistor to respond to the input signal.

## V. Conclusions

In this paper, a new technique for solving the HDM in conjunction with Poisson's equation using an adaptive real-coded GA has been developed. Several GA design parameters have been studied to illustrate their effects on the algorithm convergence. The novelty of the proposed technique comes from the GA itself. This has been achieved by developing a very efficient objective function along with introducing completely new concepts such as fitness-dependent GA parameters. Moreover, the problem this paper has presented is a new application for GAs. In addition, the proposed GA will outperform standard methods for several types of problems. For instance, finding the global solution of optimization problems having multiple local minima and problems where matrices have large condition numbers. This paper also represents a fundamental step toward applying GAs to Maxwell's equations in conjunction with the HDM, aiming to develop an optimized and unconditionally stable global-modeling simulator.

## References

[1] S. El-Ghazaly and T. Itoh, "Electromagnetic interfacing of semiconductor devices and circuits," in *IEEE MTT-S Int. Microwave Symp. Dig.*, 1997, pp. 151–154.

[2] S. M. S. Imtiaz and S. M. El-Ghazaly, "Global modeling of millimeter-wave circuits: Electromagnetic simulation of amplifiers," *IEEE Trans. Microwave Theory Tech.*, vol. 45, pp. 2208–2216, Dec. 1997.

[3] M. A. Alsunaidi, S. M. Imtiaz, and S. M. El-Ghazaly, "Electromagnetic wave effects on microwave transistors using a full wave high-frequency time-domain model," *IEEE Trans. Microwave Theory Tech.*, vol. 44, pp. 799–808, June 1996.

[4] R. O. Grondin, S. M. El-Ghazaly, and S. Goodnick, "A review of global modeling of charge transport in semiconductors and full-wave electromagnetics," *IEEE Trans. Microwave Theory Tech.*, vol. 47, pp. 817–829, June 1999.

[5] Y. Rahmat-Samii and E. Michielssen, *Electromagnetic Optimization by Genetic Algorithms*. New York: Wiley, 1999.

[6] T. Itoh and T. Nishino, "Evolutionary generation of microwave line-segment circuits by genetic algorithms," *IEEE Trans. Microwave Theory Tech.*, vol. 50, pp. 2048–2055, Sept. 2002.

[7] S. Chakravarty, R. Mittra, and N. R. Williams, "On the application of the microgenetic algorithm to the design of broad-band microwave absorbers comprising frequency-selective surfaces embedded in multilayered dielectric media," *IEEE Trans. Microwave Theory Tech.*, vol. 49, pp. 1050–1059, June 2001.

[8] J. Haala, W. Wiesbeck, and T. Zwick, "A genetic algorithm for the evaluation of material parameters of compound multilayered structures," *IEEE Trans. Microwave Theory Tech.*, vol. 50, pp. 1180–1187, Apr. 2002.

[9] Z. Chen and L. Guo, "Application of the genetic algorithm in modeling RF on-chip inductors," *IEEE Trans. Microwave Theory Tech.*, vol. 51, pp. 342–346, Feb. 2003.

[10] E. Michielssen, R. Mittra, S. Ranjithan, and J.-M. Sajer, "Design of lightweight, broad-band microwave absorbers using genetic algorithms," *IEEE Trans. Microwave Theory Tech.*, vol. 41, pp. 1024–1031, June 1997.

[11] C. Chien-Ching and C. Wei-Ting, "Electromagnetic imaging for an imperfectly conducting cylinder by the genetic algorithm," *IEEE Trans. Microwave Theory Tech.*, vol. 48, pp. 1901–1905, Nov. 2000.

[12] D. A. Coley, *An Introduction to Genetic Algorithms for Scientists and Engineers*. New York: World Sci., 1999.

[13] C. Hilsum, "Simple empirical relationship between mobility and carrier concentrations," *Electron Lett.*, vol. 10, no. 12, pp. 259–260, 1974.

[14] J. W. Demmel, *Applied Numerical Linear Algebra*. Philadelphia, PA: SIAM, 1997.

**Yasser A. Hussein** (M'03) was born in Cairo, Egypt. He received the B.S. and M.S. degrees in electrical engineering from Cairo University, Cairo, Egypt, in 1995 and 1998, respectively, and the Ph.D. degree in electrical engineering from Arizona State University, Tempe, in 2003.

He has been with several universities and research centers including Cairo University, the National Institute of Standardization (NIS), Cairo, Egypt, and Arizona State University. He is currently with the Stanford Linear Accelerator Center (SLAC), Stanford University, Menlo Park, CA. His current research interests are in the areas of computer-aided design of microwave integrated circuits, computational electromagnetics and semiconductor high-frequency RF modeling and measurements, and wireless communications.

Dr. Hussein is an elected member of the National Society of Collegiate Scholars and Phi Kappa Phi.

**Samir M. El-Ghazaly** (S'84–M'86–SM'91–F'01) received the Ph.D. degree in electrical engineering from the University of Texas at Austin, in 1988.

In August 1988, he joined Arizona State University, and became a Professor in 1998. He is currently the Department Head of Electrical and Computer Engineering, University of Tennessee, Knoxville. He has visited and been with several universities and research centers including Cairo University, Cairo, Egypt, the Centre Hyperfrequences et Semiconducteurs, Université de Lille I, Lille, France, the University of Ottawa, Ottawa, ON, Canada, the University of Texas at Austin, NASA's Jet Propulsion Laboratory, Pasadena, CA, CST-Motorola Inc., Tempe, AZ, Institut d'Electronique de Microélectronique et de Nanotechnologie (IEMN), Université de Lille, and the Swiss Federal Research Institute (ETH), Zurich, Switzerland. His research interests include RF and microwave circuits and components, microwave and millimeter-wave semiconductor devices, semiconductor device simulations, ultrashort pulse propagation, microwave-optical interactions, linear and nonlinear modeling of superconductor microwave lines, wave–device interactions, electromagnetics, and numerical techniques applied to MMICs.

Dr. El-Ghazaly is a member of Tau Beta Pi, Sigma Xi, and Eta Kappa Nu. He is an elected member of Commissions A and D, URSI. He was the secretary and vice chairman, and is currently the chairman of Commission A, U.S. National Committee of URSI. He is a member of the Technical Program Committee for the IEEE Microwave Theory and Techniques Society (IEEE MTT-S) International Microwave Symposium (IMS) since 1991. He is on the Editorial Board of the IEEE TRANSACTIONS ON MICROWAVE THEORY AND TECHNIQUES. He was the chairman of the IEEE Waves and Devices Group, Phoenix Section. He was the chapter funding coordinator and chairman of the Chapter Activities Committee of the IEEE MTT-S. He is an elected member of the Administrative Committee of the IEEE MTT-S. He is the editor-in-chief of the IEEE MICROWAVE AND WIRELESS COMPONENTS LETTERS. He was the general chairman of the IEEE MTT-S 2001 IMS, Phoenix, AZ, May 2001.